Stark fluorescence spectroscopy on peridinin–chlorophyll–protein complex of dinoflagellate, Amphidinium carterae

Ara, Anjue Mane; Shakil Bin Kashem, Md; van Grondelle, Rienk; Wahadoszamen, M.D.

published in
Photosynthesis Research
2020

DOI (link to publisher)
10.1007/s11120-019-00688-9

document version
Publisher's PDF, also known as Version of record

Photosynthesis Research (2020) 143:233–239
https://doi.org/10.1007/s11120-019-00688-9

ORIGINAL ARTICLE

Stark fluorescence spectroscopy on peridinin–chlorophyll–protein complex of dinoflagellate, *Amphidinium carterae*

Anjue Mane Ara[1,2] · Md. Shakil Bin Kashem[2] · Rienk van Grondelle[1] · Md. Wahadoszamen[1,3]

Received: 18 August 2019 / Accepted: 30 October 2019 / Published online: 25 November 2019

Abstract

Because of their peculiar but intriguing photophysical properties, peridinin–chlorophyll–protein complexes (PCPs), the peripheral light-harvesting antenna complexes of photosynthetic dinoflagellates have been unique targets of multidimensional theoretical and experimental investigations over the last few decades. The major light-harvesting chlorophyll *a* (Chl *a*) pigments of PCP are hypothesized to be spectroscopically heterogeneous. To study the spectral heterogeneity in terms of electrostatic parameters, we, in this study, implemented Stark fluorescence spectroscopy on PCP isolated from the dinoflagellate *Amphidinium carterae*. The comprehensive theoretical modeling of the Stark fluorescence spectrum with the help of the conventional Liptay formalism revealed the simultaneous presence of three emission bands in the fluorescence spectrum of PCP recorded upon excitation of peridinin. The three emission bands are found to possess different sets of electrostatic parameters with essentially increasing magnitude of charge-transfer character from the blue to redder ones. The different magnitudes of electrostatic parameters give good support to the earlier proposition that the spectral heterogeneity in PCP results from emissive Chl *a* clusters anchored at a different sites and domains within the protein network.

Keywords Light harvesting · Energy transfer · Peridinin–chlorophyll–protein complexes · Charge-transfer states · Stark spectroscopy · Spectral heterogeneity

Introduction

About 40% of photosynthesis on earth occurs in aquatic environments. Aquatic photosynthetic systems exhibit a great genetic diversity that is manifested in a large variety of photosynthetic apparatuses. Photosynthetic dinoflagellates, a class of phytoplankton, possess a unique photosynthetic apparatus that extensively uses both carotenoids and chlorophylls (Chls) as the main light harvesters (Carbonera et al. 2014). Dinoflagellates contain a membrane-bound light-harvesting complex similar to that of higher plants. In addition, they have developed a water-soluble peripheral antenna, peridinin–chlorophyll–protein (PCP), which has no sequence similarity with other known photosynthetic proteins. Dinoflagellates use peridinin as their predominant carotenoid to supplement light capture in the spectral region of maximal solar irradiance from 420 to 550 nm.

PCP is a very robust and unique antenna system where the bound carotenoids stochiometrically outnumber the Chls. The structure of PCP of the dinoflagellates species *Amphidinium carterae* (*A. carterae*) (Hofmann et al. 1996) displays a supramolecular structure which consists of two symmetric domains, each with a central Chl *a* surrounded by four peridinin molecules and embedded in a protein matrix. Upon light absorption, peridinins in PCP transfer their electronic excitation to Chl *a* with an exceptionally high (close to 100%) efficiency (Song et al. 1976). In the literature, the pathways of excited state energy transfer and relaxation in PCP were studied by many authors through different ways (Bonetti et al. 2010; Damjanović et al. 2000; Kleima et al. 2000; Steck et al. 1990; Krikunova et al. 2006).

Electronic supplementary material The online version of this article (https://doi.org/10.1007/s11120-019-00688-9) contains supplementary material, which is available to authorized users.

✉ Md. Wahadoszamen
wahado.phy@du.ac.bd

[1] Biophysics of Photosynthesis, Department of Physics and Astronomy, Faculty of Sciences, VU University Amsterdam, Amsterdam, The Netherlands

[2] Department of Physics, Jagannath University, Dhaka 1100, Bangladesh

[3] Department of Physics, University of Dhaka, Dhaka 1000, Bangladesh

A comprehensive study shows that the energy levels of peridinin found in PCP consist of two singlet excited states S_1 and S_2 which are energetically higher than and close to the Chl *a* Q_y and Q_x excited states. Upon light absorption, peridinins are in general excited to their optically allowed S_2 state. The excitation energy from the S_2 is believed to follow three distinct pathways to reach the Chl *a* Q_y state: (i) it is directly funneled to Chl *a* on an ultrafast timescale in competition with internal conversion to low-lying optically forbidden states (i.e., S_1 state) of peridinin, (ii) it is at first transferred to the optically forbidden S_1 state via internal conversion, and then finally transferred to the Q_y state of Chl *a*, (iii) it follows an additional route via the S_1—ICT mixed state to reach the Q_y state of Chl *a*, (Zigmantas et al. 2002; Bonetti et al. 2010; Damjanović et al. 2000; Kleima et al. 2000; Krikunova et al. 2006; Steck et al. 1990). According to the literature, the populated Q_y state of Chl *a* ultimately passes energy to the membrane-bound PSII complex: this transfer could occur via the interplay of LHC*a/c* complex II or CP43 or CP47 complexes (Mimuro et al. 1990), or directly to the PSII core complex (Knoetzel and Rensing 1990). From the intrinsic construction of chlorophyll–carotenoid protein, it is suggested that both the PCP and LHC can coexist in a stacked configuration and hence constitute a suitable channel for downhill energy transfer. It is also proposed that highly efficient Förster energy transfer from PCP to LHC can be expected, because the tetrapyrrole rings of their chlorophylls would be approximately coplanar (Kleima et al. 2000).

Besides the light-harvesting role, peridinin in PCP is suggested to confer a significant role to quench harmful photo-oxidizing singlet oxygen that arises as an unwanted by-product during photosynthesis. When the number of Chl *a* excited singlet states is too numerous and unable to be transferred to the membrane-bound antenna complexes, Chl *a* triplet states form, which then sensitize the formation of deleterious photo-oxidizing singlet oxygen (Alexandre et al. 2007). Peridinin quenches such singlet oxygen and thereby chlorophyll triplet excitations and thus preserves the structural and functional integrity of the photosynthetic apparatus. The quenching reaction involves triplet excitation transfer from chlorophyll to peridinins.

After the pioneering works of Song and coworkers (Song et al. 1976), PCPs have been the subject of intensive research works over the last few decades. PCPs possess peculiar but intriguing photophysical properties. Hence, PCPs have been a unique target of multidimensional research endeavors evolved so far with various experimental techniques with the ultimate objective to better elucidate their photophysical properties (Alexandre et al. 2007; Carbonera et al. 2014; Damjanović et al. 2000; Garab and Breton 1976; Hofmann et al. 1996; Iglesias-Prieto et al. 1991; Iglesias-Prieto and Trench 1996; Kleima et al. 2000; Knoetzel and Rensing 1990; Krikunova et al. 2006; Mimuro et al. 1990; MURATA 1986). In the present study, we applied Stark fluorescence (SF) spectroscopy to PCP of the dinoflagellates species *Amphidinium carterae* with the aim to better characterize the emitting specie(s) associated with fluorescence more specifically by uncovering their excited state electronic structure and dynamics. The precise knowledge about the nature of PCP fluorescence is essential since a clear understanding about the pathways and mechanisms that PCPs follow for deactivating their singlet exciton energy via fluorescence is still nebulous. Stark spectroscopy, which monitors electric field-induced changes in absorption (Stark absorption, SA) or fluorescence (Stark fluorescence, SF), can be used to probe and quantify the change in electrostatic parameters such as permanent dipole moment and molecular polarizability following optical excitation and/or relaxation (Wahadoszamen et al. 2007, 2012, 2014a, b, 2015; Ara et al. 2006, 2007; Bublitz and Boxer 1997), as well as to probe the rates of excited state reactions and deactivations and their response to an electric field (Wahadoszamen et al. 2014b). The determination of these parameters is essential for the characterization of the excited state electronic structures and dynamics of the molecule or molecular aggregate under study. Stark spectroscopy is particularly useful for the identification of charge-transfer (CT) states since CT states are typically associated with a large electric dipole moment and thus exhibit highly selective and sensitive response to the externally applied electric field during the course of experiment (Wahadoszamen et al. 2012, 2014a, b; Nakabayashi et al. 2005). Stark spectroscopy is also a very useful tool to unravel the spectral constituents of different spectral species or aggregates coexisting within an ensemble, which, because of having closely lying energy levels, yields a single spectral profile in conventional spectroscopy (Ara et al. 2006; Wahadoszamen et al. 2016).

Materials and methods

PCP from *A. carterae* was prepared as described in ref *Hoffmann* (2). The Stark sample of PCP was prepared by suspending it in a buffer containing 25 mM Tris of pH 7.5, 2 mM KCl, and 0.06% β-DDM and subsequently mixed with glycerol at 60% (v/v) for making transparent glass at 77 K. The OD of the PCP sample recorded through the Stark cell (which consists of a pair of ITO-coated quartz plates joined by 100-µm double-sided sticky tape) at 77 K was 0.22 at the peak of Q_y absorption band of Chl *a* (i.e., at 667 nm). The SF spectroscopy was carried out at 77 K in a custom-built setup, as described earlier in (Wahadoszamen et al. 2014c, 2016). The SF experimental technique relies on the simultaneous detection of F and modulated SF signals through a lock-in amplifier (SR850

in our case) typically at the second harmonics of the modulation frequency. The recorded modulated SF signals are then multiplied by the factor $2\sqrt{2}$ to convert those to the equivalent dc signals. The SF spectrum is obtained by plotting the converted SF signals as a function of wavelength or wavenumber. The modeling of SF spectrum is routinely done using the standard Liptay formalism, the details of which can be found elsewhere in the literature (Bublitz and Boxer 1997; Wahadoszamen et al. 2014c, 2016). According to the standard Liptay approach, the SF spectrum (which is often regarded as the difference between the fluorescence spectra taken with and without electric field) recorded from a random distribution of spatially fixed emitting chromophores maintaining negligible (inter-chromophore) excitonic interactions can often be approximated as the weighted superposition of the zeroth-, first-, and second-order derivatives of the F spectrum measured without electric field:

$$\frac{2\sqrt{2}\Delta F(\nu)}{F_{\max}} = \left(fF_{\text{ext}}\right)^2 \left\{ A_\chi F(\nu) + B_\chi \nu^3 \frac{d\left[F(\nu)/\nu^3\right]}{d\nu} + C_\chi \nu^3 \frac{d^2\left[F(\nu)/\nu^3\right]}{d\nu^2} \right\} \tag{1}$$

where $F_{\max}$ is the maximum F intensity, F_{ext} is the amplitude of the externally applied electric field, χ is the experimental angle between the direction of F_{ext} and the electric polarization of the excitation light of energy ν, and f is the local field correction factor that relates the F_{ext} with the internal electric field (F_{int}) experienced by the chromophore $\left(F_{\text{int}} = fF_{\text{ext}}\right)$. The weight of the zeroth-order derivative gives an estimate of the field-induced change in emission intensity arising mostly from field-induced modulation of the rates of the associated nonradiative deactivations. Besides, the weights of the first and the second derivatives often provide crucial information about the electronic structure, more specifically changes in electrostatic parameters such as molecular polarizability ($\Delta\alpha$) and dipole moment ($\Delta\mu$) between the ground and excited states upon F transition, respectively. At magic angle ($\chi = 54.7°$), the coefficients B_χ and C_χ can be expressed as:

$$B_{54.7°} = \frac{\Delta\alpha}{2hc} \tag{2}$$

$$C_{54.7°} = \frac{(\Delta\mu)^2}{6h^2c^2}. \tag{3}$$

Therefore, upon reproducing the shape of SF spectrum with a linear superposition of the derivatives of the respective F spectrum and computing the coefficients of the first and second derivatives, one can extract the values of $\Delta\alpha$ and $\Delta\mu$ from the above two equations.

Result and analysis

The upper and lower panels of Fig. 1 present, respectively, the F and SF spectra (measured at 77 K) of isolated PCP obtained from the dinoflagellate *A. carterae*. The F and SF spectra of PCP are denoted hereafter as F PCP and SF PCP, respectively. Both the F PCP and SF PCP signals are recorded simultaneously with an excitation wavelength of 469 nm where the sample has negligible SA signal (the SA spectrum is displayed in Fig. s1 of ESI). The SF spectrum is scaled to the field strength of 1 MV cm^{-1}, although multiple SF spectra were measured within the range from 0.30 to 0.40 MV cm^{-1}. Scaling SF spectra to 1 MV cm^{-1} greatly simplifies the mathematical expressions used for evaluating the electrostatic parameters from the outcome of the theoretical modeling. The F PCP exhibits a characteristic sharp and well-defined emission band with a peak at 670 nm, accompanied by a vibrational progression with a peak at around 728 nm in the longer wavelength region. The F spectrum of PCP is found to be identical to that reported elsewhere (Iglesias-Prieto and Trench 1996). In the SF PCP, on the other hand, the characteristic sharp band shows negative intensity

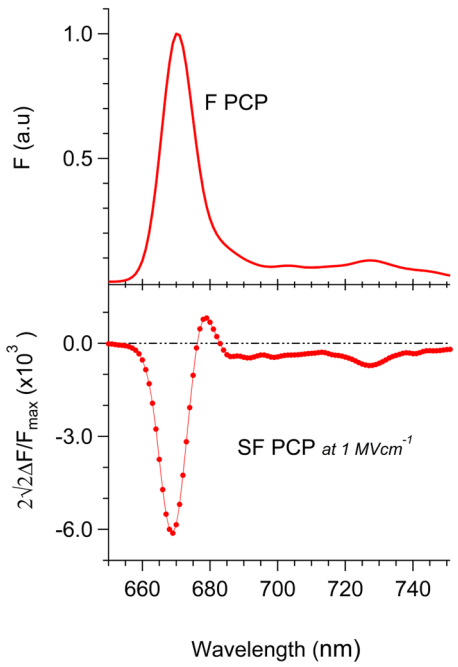

Fig. 1 F (top) and SF (bottom) spectra of PCP recorded simultaneously at 77 K with excitation at 469 nm. The SF spectrum reported in the figure is scaled to the field strength 1 MV cm^{-1} and normalized to the maximum intensity of the F

with a peak at 669 nm and a positive hump at around 679 nm and the remaining spectrum shows negative amplitude with a shape seemingly identical to that of the F spectrum. In addition, the SF peak of PCP is found to be shifted by 1 nm compared to its F peak suggesting that the field-induced peak shift in the SF spectrum is rather small.

According to the standard Liptay formalism as discussed above, the SF spectrum in a certain wavelength window can reasonably be reproduced by a weighted superposition of the zeroth-, first- and second-order derivatives of the observed F spectrum without deconvolution (Bublitz and Boxer 1997; Wahadoszamen et al. 2007, 2014b, 2016). This theoretical hypothesis can yield a realistic fit of the SF spectrum throughout the spectral window of interest when the SF originates from a single type of noninteracting photoactive chromophores (Nakabayashi et al. 2005). However, if the SF spectrum is composed of multiple types of distinct spectral species (Ara et al. 2006; Wahadoszamen et al. 2012, 2016), the linear superposition of the derivatives of the observed F spectrum (without deconvolution) cannot yield a plausible fit of SF spectrum throughout the spectral window under consideration, but often yields a lineshape that deviates significantly from the SF spectrum around some regions. In such a case, the observed F spectrum needs to be deconvoluted into a set of bands representing the emission signatures of the available multiple species. The weighted sum of the derivatives of the deconvoluted bands can then be employed to obtain a satisfactory fit of the SF spectrum (Wahadoszamen et al. 2012, 2016). Therefore, to test the contribution of multiple spectral species, we, in a first trial, attempted to reproduce the SF PCP by a linear superposition of the zeroth-, first- and second-order derivatives of the overall F PCP without deconvolution. The resulting fit (solid blue line) is shown together with the SF spectrum (circled red line) in Fig. 2. One can easily notice that although the fit has a good match with the SF spectrum in the 670 nm region, however, a small but clear mismatch is readily apparent both in the shorter and in the longer wavelength regions around 654–662 nm, 680–705 nm, and 720–750 nm. In line with the aforementioned hypothesis, the clear mismatches essentially reflect the SF contribution of some additional species whose emission signatures are somehow hidden underneath the major emission band. To this end, the mismatch in the shorter wavelength region is most likely to result from some small fraction of free Chl *a* available in PCP preparation. The observed intensity in the shorter wavelength tail of F PCP can thus be considered to be a superposition of F emission coming from both bound Chl *a* and free Chl *a*, and it is very much expected that emission of free Chl *a* would experience a different magnitude of modulation by the electric field compared to the bound Chl *a*. As the free Chl *a* is not the focus of this study, we will not consider its contribution in our discussion hereafter. Then, the mismatch around

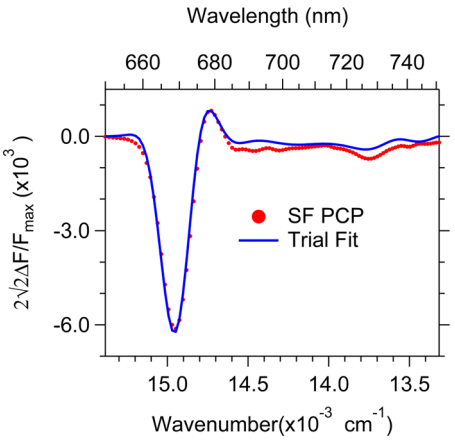

Fig. 2 SF PCP (circled red line) and Trial Fit (solid blue line) obtained by the linear superposition of the derivatives of the observed F PCP without deconvolution

the mid (680–705 nm) and the longer (720–750 nm) wavelength regions most likely arises from the interplay of two additional spectral species that yielded different magnitudes of the SF signal compared to the one associated with the major (670 nm) emission band. The two new spectral species are likely to be characterized by weak emission yields and hence are largely hidden beneath the vibrational tail of the major 670 nm emission band. However, it can also be possible that the three spectral species are associated with very different excited state electronic structures and dynamics and thus capable of exhibiting a selective response to the electric field. Due to their selective response to the electric field, the signatures of the two new species could be evident in the SF spectrum. Therefore, it is clear that the SF PCP is mainly characterized by a main band peaking at 670 nm: however, at least two new bands need to be considered in order to achieve a satisfactory fit in the regions of deviations at around 680–705 nm and at 720–750 nm. To this end, one may anticipate that the disagreement between the fit and SF spectrum around the longer wavelength region above 720 nm may arise from the incapability of the standard Liptay formalism to deal with the SF signals around the region of the vibrational satellite. However, the implementation of a similar protocol to model the SF data of other photosynthetic antenna complexes (unpublished data) shows that Liptay formalism is capable to produce a plausible fit around the vibrational satellite as well (see Fig. s2 of ESI).

With the information obtained above at hand, the F spectrum of PCP was deconvoluted into three bands b1, b2, and b3 having peaks, respectively, at 670 nm, 684 nm, and 727 nm as shown in Fig. 3 where b1 represents the main emission band and the remainder (b2 and b3) are the two new bands introduced around the regions of mismatch. The b1 band shape is synthesized by the weighted superposition

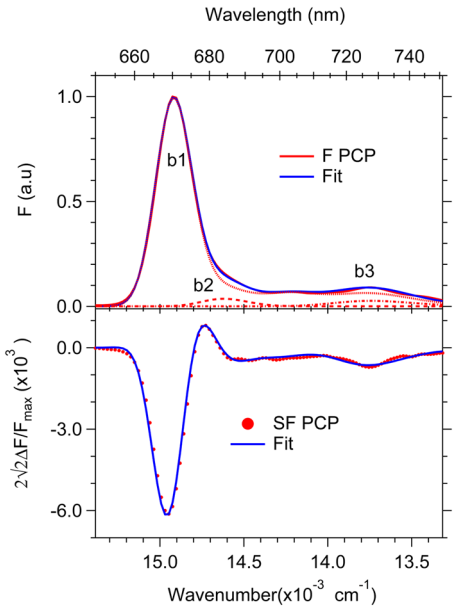

Fig. 3 (Top) F PCP (solid red line) and its fit (solid blue line). The fit is obtained with linear superposition of some skewed Gaussians. The F spectrum is then deconvoluted into three constituent bands (b1, b2, and b3) of varying skewness and width peaking at 670, 684, and 727 nm. The deconvolution is done in such a manner that they can yield plausible simultaneous fit of the F and SF spectra. (Bottom) SF (circled red line) spectrum and the resulting fit (solid blue line) obtained with the weighted superposition of the derivatives of the deconvoluted bands

Table 1 Estimated molecular parameters for PCP

Band	λ_{max} (nm)	Bandwidth (nm)	ZDC (at 1 MV cm^{-1})	$\Delta\alpha$ [Å^3/f^2]	$\Delta\mu$ [D/f]
b1	670	12	−0.004	13	0.5
b2	684	15	0.001	−72	1.0
b3	727	27	−0.01	−18	1.6

All the parameters are within 10% standard error

ZDC zeroth derivative contribution

of multiple skewed Gaussian functions having variable skewness, bandwidth, and intensity, while the b2 and b3 bands were produced by two distinct single skewed Gaussian functions with peaks at 684 and 727 nm. In this deconvolution protocol, the b1 band was assumed to be the major emission profile of PCP and therefore the band was ornamented with the broad vibrational tail. The linear superposition of the derivatives of all the deconvoluted bands was then employed to model the SF spectrum. The bottom panel of the Fig. 3 displays the results of the modeling. One can easily notice from the figure that such deconvolution-associated modeling could yield a plausible fit of the SF spectrum throughout the wavelength region of interest. The molecular parameters evaluated from the derivative contributions of the deconvoluted bands are complied in Table 1.

We see from the table that, for b1 of F PCP, the analysis yields nonzero zeroth derivative contribution (ZDC) (−0.004 at a field strength of 1 MV cm^{-1}), $\Delta\alpha$ (13 [Å^3/f^2]), and $\Delta\mu$ (0.5 [D/f]). The obtained small magnitude of ZDC together with its negative sign indicates that the applied electric field makes the rates of the associated nonradiative deactivation slightly larger compared to those corresponding to radiative deactivation. The rather small value of estimated $\Delta\mu$ indicates that the state associated with the b1 band has little CT character. For b2 of F PCP, the analysis yields nonzero ZDC (0.001 at a field strength of 1 MV cm^{-1}), $\Delta\alpha$ (−72 [Å^3/f^2]), and Δμ (1.0 [D/f]). The estimated small positive ZDC value indicates that the emission yield of the b2 band is slightly enhanced by the applied electric field. However, the larger values of the estimated Δμ suggest that the state associated with the b2 band has slightly larger CT character compared to that of b1. On the other hand, for b3 of F PCP, the analysis yields the values of ZDC, Δα, and Δμ of -0.01 at a field strength of 1 MV cm^{-1}, − 18 [Å^3/f^2]), and 1.6 [D/f]), respectively. Therefore, as far as the magnitude of Δμ is concerned, the emitting state of b3 possesses threefold larger CT character compared to that of b1.

Discussion

The overall absorption spectrum of PCP typically covers the region from 450 to 670 nm: the absorption in the 450-600 nm region is due to peridinin; at 430 nm, it is due to the Soret band of Chl *a;* and at 670 nm, it is due to the Q_y band of Chl *a* (Kleima et al. 2000). On the other hand, the F PCP exhibits a characteristic sharp and well-defined emission band (appearing from Chl *a*) with a peak at 670 nm, accompanied by a vibrational tail with a peak at around 728 nm in the longer wavelength region even when the excitation wavelength (469 nm) was in the peridinin absorption region. Though excitation wavelength was in peridinin absorption region, the emission observed at 670 nm Q_y band of Chl *a* implies that light energy absorbed by peridinin induces significant Chl *a* fluorescence by efficient intramolecular energy transfer (Song et al. 1976). However, the well-defined emission lineshape obtained from PCP does not represent the spectral signature of a single type of Chl *a*, since Chl *a* chromophores embedded within PCP protein matrix are proven to be spectroscopically heterogeneous. To this end, from the Gaussian deconvolution of emission spectra followed by a controlled temperature dependence study, Iglesias-Prieto et al. could clearly identify the existence of two distinct spectral species of Chl *a* in PCP (Iglesias-Prieto and Trench 1996). The observed spectral heterogeneity was suggested to be the result from both the spatial and functional

heterogeneity within the host protein structure which in turn confers different magnitudes of perturbation to the electronic state of encapsulated Chls *a* via the combined interplay of different interactions (Iglesias-Prieto and Trench 1996). Besides, it is also hypothesized that the different spectral species of Chl *a* in PCP originate either from a monomeric or from a dimeric PCP where the two Chl *a* pigments are encapsulated along with 4/5 peridinin in the monomeric or dimeric apoprotein (Iglesias-Prieto et al. 1991).

In line of such thinking, it seems very likely that the three emission bands resolved in this study reflect the emission signatures of three distinct spectral species of Chl *a* generated due to their placement at different locations within the host protein matrix. In the Q_y absorption region of PCP from *A. carterae*, two sub-bands (related to the two Chl *a* of each monomer) have been partly resolved at cryogenic temperatures (Murata 1986; Garab and Breton 1976). Moreover, two different C=O stretching modes (1697 and 1681 cm^{-1}) were observed by fluorescence line-narrowing spectroscopy, suggesting that there are two different emitting Chls *a* (Garab and Breton 1976). A Gaussian deconvolution of the RT fluorescence emission spectrum of PCP from *Symbiodinium microadriaticum* revealed two well-separated emission bands centered at 675.5 and 679 nm (Iglesias-Prieto et al. 1991; Iglesias-Prieto and Trench 1996). The site energies of the attached chromophores (peridinins as well as Chls *a*) may differ in the C- and N-terminal clusters since amino-acid sequences of the C- and N-terminal regions of the PCP apoprotein are only ~56% identical. The site energies of the four peridinins within one cluster are also expected to vary because of their different attachment sites in the protein matrix. These may be the reasons why the signatures of spectroscopically different Chls *a* in PCP were observed through different experiments. In line with the previous available information, we can assume that the emission bands b1 and b2 within the main emission band may come from two Chls *a* associated either with monomeric or with dimeric PCP. Note that the molecular parameters of b2 ($\Delta\alpha = -72$ [$Å^3/f^2$] and ($\Delta\mu = 1.0$ [D/f]) are larger than those of b1 ($\Delta\alpha = 13$ [$Å^3/f^2$] and $\Delta\mu = 0.5$ [D/f]) confirming that two different emitting Chls *a* clusters (be it within monomeric or dimeric PCP apoprotein) interact with their environment differently thereby yielding two different emitting bands of Chls *a* at two different frequencies.

However, the band b3 seems to be the additional band resolved through the unique usefulness of SF spectroscopy. The analysis yielded a large magnitude of ZDC for the b3 band and essentially a three-fold larger magnitude of Δμ compared to the b1 band. Moreover, the band b3 has significantly large magnitude of bandwidth and Stokes shift. The large magnitude of Stokes shift and bandwidth of b3 band may reflect a large extent of electron–phonon coupling and interaction among the interacting emissive pigments in a specific site within the protein matrix. If it is so, like for other photosynthetic pigment–protein complexes, the F state of b3 could be mixed with a nearby charge-transfer (CT) state and hence inherited with a larger CT character (Wientjes et al. 2012). The estimated fairly larger magnitude of the estimated Δμ gives some support to this proposition.

Conclusion

By applying SF spectroscopy, we could identify the simultaneous presence of three emissive spectral species of Chl *a* in PCP isolated from the dinoflagellate *Amphidinium carterae*. The comprehensive analysis of the SF spectrum yielded different sets of electrostatic parameters for the three spectral species. The different electrostatic parameter may arise from the Chl *a* clusters arranged at different sites and domains within the protein web, which may confer the Chl *a* to assume different structural geometries and/or exposure to different functional groups. If so happens, it would not be an unusual expectation that Chl *a* will acquire different electronic structures and dynamics at different sites and domains of the protein interior. The different sets electrostatic parameters obtained for the deconvoluted bands supports very well this hypothesis. Therefore, it seems very likely that pigment–protein interaction plays major role in inducing CT character to Chl *a* and to the variation of its other electrostatic properties within PCP. Moreover, larger magnitudes of Δμ for the longer wavelength bands (especially for the b3) together with their larger bandwidths may point to the additional role of peridinin in inducing CT character in Chl *a*. PCP is a very robust and flexible pigment–protein complex that presumably performs crucial photosynthetic functions associated with both efficient light harvesting and photoprotection. The identified multiple emissive species may confer PCP to perform such diverse functions and hence providing it unique functional plasticity.

Improved understanding about the excited state photophysics of PCP in natural light-harvesting systems is critical for designing efficient artificial mimics thus to engineer robust artificial photosynthetic systems for solar energy conversion and storage. The peculiar photophysical properties of PCP have suggested their use in technological perspective, for example, in the field of hybrid nanostructures for light energy conversion, and as a tool for emission enhancement of PCPs as a fluorophore in biomedical studies, as a possible anti-cancer role.

Acknowledgements Md. W., A. M. A., and R. v. G. were supported by the VU University Amsterdam, the Laserlab-Europe Consortium and the advanced investigator Grant (267333, PHOTPROT) from the European Research Council. Md. W. and R. v. G. were supported further by

the TOP grant (700.58.305) from the Foundation of Chemical Sciences part of NWO.

Compliance with ethical standards

Conflict of interest The authors declare that they have no conflict of interest.

References

Alexandre MT, Lührs DC, Van Stokkum IH, Hiller R, Groot M-L, Kennis JT, Van Grondelle R (2007) Triplet state dynamics in peridinin-chlorophyll-a-protein: a new pathway of photoprotection in LHCs? Biophys J 93(6):2118–2128

Ara AM, Iimori T, Yoshizawa T, Nakabayashi T, Ohta N (2006) External electric field effects on fluorescence of pyrene butyric acid in a polymer film: concentration dependence and temperature dependence. J Phys Chem B 110(47):23669–23677

Ara AM, Iimori T, Nakabayashi T, Maeda H, Mizuno K, Ohta N (2007) Electric field effects on absorption and fluorescence spectra of trimethylsilyl-and trimethylsilylethynyl-substituted compounds of pyrene in a PMMA film. J Phys Chem B 111(36):10687–10696

Bonetti C, Alexandre MT, van Stokkum IH, Hiller RG, Groot ML, van Grondelle R, Kennis JT (2010) Identification of excited-state energy transfer and relaxation pathways in the peridinin–chlorophyll complex: an ultrafast mid-infrared study. Phys Chem Chem Phys 12(32):9256–9266

Bublitz GU, Boxer SG (1997) Stark spectroscopy: applications in chemistry, biology, and materials science. Annu Rev Phys Chem 48(1):213–242

Carbonera D, Di Valentin M, Spezia R, Mezzetti A (2014) The unique photophysical properties of the Peridinin-Chlorophyll-a-Protein. Curr Protein Pept Sci 15(4):332–350

Damjanović A, Ritz T, Schulten K (2000) Excitation transfer in the peridinin-chlorophyll-protein of *Amphidinium carterae*. Biophys J 79(4):1695–1705

Garab GI, Breton J (1976) Polarized light spectroscopy on oriented spinach chloroplasts fluorescence emission at low temperature. Biochem Biophys Res Commun 71(4):1095–1102

Hofmann E, Wrench PM, Sharples FP, Hiller RG, Welte W, Diederichs K (1996) Structural basis of light harvesting by carotenoids: peridinin-chlorophyll-protein from *Amphidinium carterae*. Science 272(5269):1788–1791

Iglesias-Prieto R, Trench R (1996) Spectroscopic properties of chlorophylla in the water-soluble peridinin-chlorophylla-protein complexes (PCP) from the symbiotic dinoflagellate *Symbiodinium microadriaticum*. J Plant Physiol 149(5):510–516

Iglesias-Prieto R, Govind N, Trench R (1991) Apoprotein composition and spectroscopic characterization of the water-soluble peridinin—Chlorophyll a—proteins from three symbiotic dinoflagellates. Proc R Soc Lond B 246(1317):275–283

Kleima FJ, Wendling M, Hofmann E, Peterman EJ, van Grondelle R, van Amerongen H (2000) Peridinin chlorophyll a protein: relating structure and steady-state spectroscopy. Biochemistry 39(17):5184–5195

Knoetzel J, Rensing L (1990) Characterization of the photosynthetic apparatus from the marine dinoflagellate *Gonyaulax polyedra*: I. Pigment and polypeptide composition of the pigment-protein complexes. J Plant Physiol 136(3):271–279

Krikunova M, Lokstein H, Leupold D, Hiller RG, Voigt B (2006) Pigment-pigment interactions in PCP of *Amphidinium carterae* investigated by nonlinear polarization spectroscopy in the frequency domain. Biophys J 90(1):261–271

Mimuro M, Tamai N, Ishimaru T, Yamazaki I (1990) Characteristic fluorescence components in photosynthetic pigment system of a marine dinoflagellate, *Protogonyaulax tamarensis*, and excitation energy flow among them. Studies by means of steady-state and time-resolved fluorescence spectroscopy. Biochim Biophys Acta BBA 1016(2):280–287

Murata N (1986) Absorption and fluorescence emission by intact cells, chloroplasts, and chlorophyll-protein complexes. In: Govindjee, Amesz J, Fork DJ (eds) Light emission by plants and bacteria. Academic Press, New York, pp 137–159

Nakabayashi T, Wahadoszamen M, Ohta N (2005) External electric field effects on state energy and photoexcitation dynamics of diphenylpolyenes. J Am Chem Soc 127(19):7041–7052

Song P-S, Koka P, Prezelin BB, Haxo FT (1976) Molecular topology of the photosynthetic light-harvesting pigment complex, peridinin-chlorophyll a-protein, from marine dinoflagellates. Biochemistry 15(20):4422–4427

Steck K, Wacker T, Welte W, Sharples FP, Hiller RG (1990) Crystallization and preliminary X-ray analysis of a peridinin-chlorophyll a protein from *Amphidinium carterae*. FEBS Lett 268(1):48–50

Wahadoszamen M, Hamada T, Iimori T, Nakabayashi T, Ohta N (2007) External electric field effects on absorption, fluorescence, and phosphorescence spectra of diphenylpolyynes in a polymer film. J Phys Chem A 111(38):9544–9552

Wahadoszamen M, Berera R, Ara AM, Romero E, van Grondelle R (2012) Identification of two emitting sites in the dissipative state of the major light harvesting antenna. Phys Chem Chem Phys 14(2):759–766

Wahadoszamen M, Ghazaryan A, Cingil HE, Ara AM, Büchel C, van Grondelle R, Berera R (2014a) Stark fluorescence spectroscopy reveals two emitting sites in the dissipative state of FCP antennas. Biochim Biophys Acta BBA 1837(1):193–200

Wahadoszamen M, Margalit I, Ara AM, Van Grondelle R, Noy D (2014b) The role of charge-transfer states in energy transfer and dissipation within natural and artificial bacteriochlorophyll proteins. Nat Commun 5:5287

Wahadoszamen M, Margalit I, Ara AM, van Grondelle R, Noy D (2014c) The role of charge-transfer states in energy transfer and dissipation within natural and artificial bacteriochlorophyll proteins. Nat Commun. https://doi.org/10.1038/ncomms6287

Wahadoszamen M, D'Haene S, Ara AM, Romero E, Dekker JP, van Grondelle R, Berera R (2015) Identification of common motifs in the regulation of light harvesting: the case of cyanobacteria IsiA. Biochim Biophys Acta BBA 1847(4):486–492

Wahadoszamen M, Belgio E, Rahman MA, Ara AM, Ruban AV, Grondelle R (2016) Identification and characterization of multiple emissive species in aggregated minor antenna complexes. Biochim Biophys Acta BBA 1857(12):1917–1924

Wientjes E, Roest G, Croce R (2012) From red to blue to far-red in Lhca4: how does the protein modulate the spectral properties of the pigments? Biochim Biophys Acta 1817(5):711–717. https://doi.org/10.1016/j.bbabio.2012.02.030

Zigmantas D, Hiller RG, Sundström V, Polívka T (2002) Carotenoid to chlorophyll energy transfer in the peridinin–chlorophyll-a–protein complex involves an intramolecular charge transfer state. Proc Natl Acad Sci USA 99(26):16760–16765